

SIMULATIONS OF UPWARD LEAKAGE OF CO₂ IN LONG-COLUMN FLOW EXPERIMENTS: EFFECT OF LATERAL BOUNDARY CONDITION

Curtis M. Oldenburg¹, Christine Doughty¹, Catherine A. Peters², and Patrick F. Dobson¹

¹Earth Sciences Division
Lawrence Berkeley National Laboratory 74-316C
Berkeley, CA 94720 USA
e-mail: cmoldenburg@lbl.gov

²Department of Civil and Environmental Engineering
Princeton University
Princeton, NJ 08544 USA

ABSTRACT

We are using TOUGH2/ECO2M to simulate CO₂ and brine flow in high-pressure long-column pressure vessels (LCPVs) that could someday be housed in an underground laboratory. The simulations are aimed at designing experiments to understand upward leakage of CO₂ from deep geologic storage, including the transition of CO₂ from super-critical to gaseous and liquid conditions. The LCPV would consist of a vertical steel pipe a few hundred meters in length and one meter in diameter with a centralized vertical pipe analogous to a well for inserting monitoring equipment. The annular region between the inner pipe and the outer wall will be filled with porous materials saturated with brine. The LCPVs would be suspended in a long vertical shaft with thermal control on the outer wall boundary. With TOUGH2/ECO2M, we are able to model all possible phase combinations of CO₂, NaCl, and water. Results for radial 2-D simulations of upward flow in the 500 m high by 1 m in diameter column are very sensitive to the choice of outer thermal boundary conditions. For the case of constant geothermal-gradient temperature on the outer wall, representing flow up a narrow flow channel such as a well, there is very little liquid CO₂ formed, as heat from the sidewall counteracts expansion cooling and the CO₂ generally remains either supercritical or gaseous. For the case of an insulated-sidewall, by which the column represents the center of a large upwelling plume, upward migration of CO₂ and related expansion cooling leads to three-phase conditions through the formation of liquid CO₂ in equilibrium with gaseous CO₂ and

brine. The lack of knowledge regarding three-phase relative permeability behavior underlines the need for large-scale flow experiments to understand multiphase CO₂ leakage.

INTRODUCTION

Concern about CO₂ leakage and associated environmental impacts from Geologic Carbon Sequestration (GCS) sites motivates research to elucidate and quantify processes governing upward flow and transport of CO₂. With only a handful of demonstration and industrial projects available, a large amount of research into the performance of GCS is carried out by numerical simulation. Beyond the well-accepted process models such as Darcy's Law for fluid flow, Fick's Law for molecular diffusion, and Fourier's Law for conductive heat transfer, there are numerous multiphase, multicomponent, and process couplings that are not as well understood and whose prediction depends to a large degree on empiricism. Progress in the understanding of hypothetical GCS processes therefore requires encoding into simulators defensible physical and chemical process models, which are often developed through laboratory experimentation.

One limitation of laboratory experiments is the length scale, which is generally restricted to bench scale with a maximum length on the order of one meter. This limitation restricts the aspects of GCS that can be tested in the laboratory. For example, large-scale upward CO₂ migration and associated depressurization would be accompanied by a large expansion as CO₂ transitions from the supercritical or liquid conditions of the storage formation to gaseous conditions at shall-

lower depths. In order to study and understand such processes and related changes in flow velocity, temperature (e.g., by expansion cooling), and trapping in the porous medium, experiments need to be conducted over long vertical length scales.

At least one CO₂-related experiment has been carried out in a long tube suspended in the stairwell of a tall building (de la Reguera et al., 2010). Slim-tube approaches used in the oil and gas industry (e.g., Maloney and Briceno, 2008) provide another method of representing a long flow path, but because slim tubes are normally deployed as tight coils, e.g., for convenience in placing them within ovens for temperature control, they do not provide a hydrostatic pressure gradient. Underground laboratories provide another opportunity for developing pressure-controlled long vertical flow columns, an approach our team has conceptualized for the “Laboratory for Underground CO₂ Investigations” (LUCI) (Peters et al., 2010).

The experiments being considered for LUCI will focus on questions such as:

- What is the extent of cooling due to decompression expansion?
- In addition to the supercritical to gas transition, can liquid CO₂ form?
- How much CO₂ becomes trapped by residual phase trapping during upward flow of CO₂?

The long-column pressure vessels (LCPVs) filled with sand and brine conceived for LUCI will be designed to represent 500 m vertical sections of the subsurface over a depth range controllable by specification of bottom and top pressure and temperature conditions. As an effectively one-dimensional system, the LCPV would formally represent either an actual one-dimensional flow path such as a leaky well (e.g., Gasda et al., 2004), or a small region in the middle of a vast upward-rising plume as sketched in Figure 1. We can control which of these scenarios we want to test through the application of different thermal boundary conditions on the outer wall of the LCPV—constant geothermal gradient temperature for the one-dimensional flow path, and insulated for the middle of a vast plume.

With an understanding developed from numerical simulations of how flow might occur in the LCPV system, precise specifications of the system can be made and used to design and build the LUCI facility. The purpose of this paper is to present simulations of experiments that could be carried out in a specific LCPV and to demonstrate the sensitivity of the formation of liquid CO₂ as supercritical CO₂ flows upwards to the choice of boundary conditions. We emphasize that this paper is not about modeling upward CO₂ and brine flow in natural systems, but rather about simulating flow and transport in a potential future LCPV. As such, the parameters and properties of the system are chosen to be those of the engineered LCPV system, not those of any natural system.

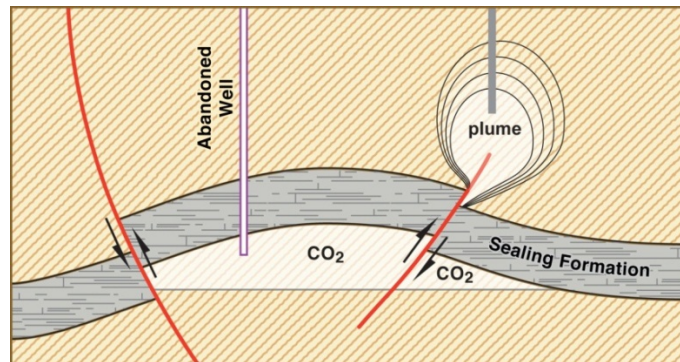


Figure 1. Conceptual models of fault and abandoned-well leakage pathways for CO₂. The one-dimensional nature of the leakage pathway is implicit in the abandoned well; for the CO₂ plume, the one-dimensional flow conceptualization is shown by the light gray bar which represents upward flow in the center of a large upwelling region.

METHODS

We carried out numerical simulations of CO₂ and brine flow in the LCPVs using TOUGH2/ECO2M (Pruess et al., 1999; Pruess, 2011). ECO2M is an equation of state module that describes the pure-component and mixture properties of water, NaCl, and CO₂. ECO2M can model the full range of phase conditions in the system H₂O-NaCl-CO₂, including P-T conditions on the liquid-gas phase boundary (saturation line) with the potential for three-phase conditions (aqueous, liquid CO₂, and gaseous CO₂). Because of its complete description of possible phase conditions, ECO2M is capable of simulating any scenario of upward CO₂ and brine flow, including the formation of liquid CO₂.

Some authors have pointed out the importance of considering the change in gravitational potential in the calculation of the enthalpy of rising fluids (e.g., Stauffer et al., 2003), a term not included in standard TOUGH2. Comparing the enthalpy change caused by pressure change from top to bottom to the gravitational potential change in the system studied here reveals that the change in gravitational potential over 500 m is insignificant relative to the pressure-volume term for the CO₂ rise scenario considered. Therefore, we can neglect the gravitational potential in the energy-balance equations.

A sketch of the long-column pressure vessel with large horizontal exaggeration is shown in Figure 2, along with the radially symmetric domain used for the simulations. The left-hand side (LHS) boundary is placed at the wall of the inner access well, which will be used for monitoring the annular flow region using various down-hole geophysical monitoring tools. This access well is currently specified to be made out of fiberglass and filled with brine under hydrostatic conditions to avoid large pressure gradients that could burst the inner wall. We assume a closed boundary (no-flow and insulated) for the inner-wall (LHS) for all of the simulations. The bottom of the LCPV is also closed and insulated, but includes flow ports such that CO₂ can be injected at a controlled rate. The top of the column is held at constant P-T conditions of 3.43 MPa and 23.75°C. These conditions correspond roughly to a depth of about 350 m in a

typical sedimentary basin. Under these conditions and with NaCl brine of 100,000 ppm concentration, the P-T at the bottom of the 500 m long LCPV are 8.67 MPa and 36.25°C. We note finally that the critical pressure and temperature for CO₂ are located at approximately -380 m and -295 m as measured downward within the LCPV, respectively.

The fixed geothermal gradient boundary condition is implemented by setting the thermal heat energy contained in the gridblocks at the boundary to an effectively infinite value (by setting either gridblock volume, rock heat capacity, or rock density to a very large value)

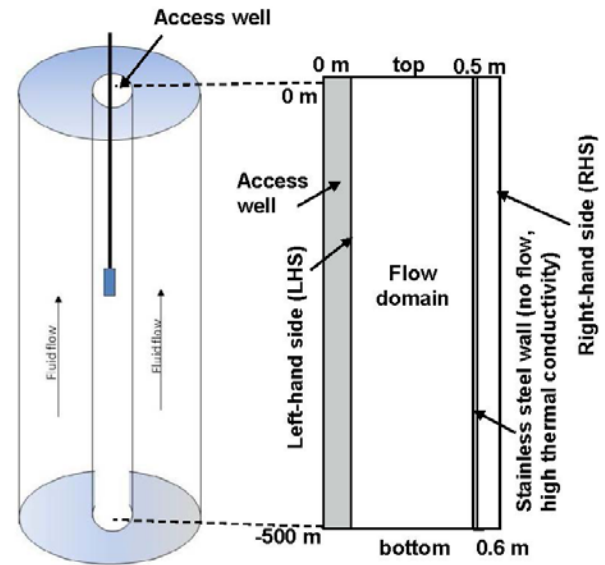


Figure 2. Sketch of annular flow region in long-column flow vessel, which includes an inner column for deployment of monitoring equipment. On the right-hand side is the two-dimensional radial numerical simulation domain with named boundaries (LHS = left-hand side (inner wall), RHS = right-hand side (outer wall)).

so that, regardless of how much heat flows into or out of the gridblock, its temperature remains the same. These fixed-temperature gridblocks are made closed to flow by setting their permeability to zero and using harmonic weighting of permeability at interfaces between gridblocks. The open boundary conditions are implemented by giving the boundary gridblocks non-zero permeability and effectively infinite volume, such that their pressures and temperatures remain constant regardless of how much fluid and heat flows in or out. The closed-to-flow and

thermally insulated boundary conditions are implemented simply by using finite-volume gridblocks with normal flow and thermal properties at the boundaries of the domain.

The model LCPV flow domain is assumed to be filled with unconsolidated sand such as one would emplace by slurry or tremie methods in the actual LCPV. The homogeneous coarse sand was chosen to allow fluid flow in the column over practical experimental time scales rather than to represent any particular sedimentary basin or reservoir system. Specific properties of the unconsolidated sand were estimated using the Rosetta Database (Schaap, 2000) which resulted in porosity, permeability, and capillary and relative permeability parameters shown in Table 1. For cases in which liquid- and gas-phase CO₂ co-exist along with aqueous-phase brine, the three-phase capillary pressure and relative permeability formulations of Parker et al. (1987) are used. The values of capillary pressure for supercritical, gaseous, and liquid CO₂ for a given aqueous-phase saturation are assumed to be the same (i.e., we assume no interfacial tension between the various phases of CO₂). The porous sand is assumed to be unreactive and immobile during all flow processes, i.e., reactive geochemistry and geomechanical stresses and deformation are neglected. We also neglect molecular diffusion because we have observed in test simulations (not presented here) its negligible effect in this high-permeability system.

Hysteretic capillary pressure and relative permeability functions are generally needed when drainage (drying) and imbibition (wetting) occur simultaneously in different parts of the flow domain. Hysteretic functions were not specified for the constant-injection case shown here because the system was expected to always remain on the drainage branch, i.e., CO₂ is injected constantly, resulting in monotonic drying processes. The fact that the constant-injection case is essentially monotonically drying is convenient, because we are not aware of the existence of a three-phase hysteretic model for CO₂-water systems.

For injection into the domain at the bottom, we assume a constant injection rate distributed in

the radial direction to produce a uniform mass flux over the bottom boundary. The total mass injection rate at the bottom of the LCPV is 1.58×10^{-2} kg/s (1.36 tonnes/d). This flow rate was derived from preliminary simulations that implemented a constant hydrostatic pressure bottom boundary, with CO₂ saturation at the boundary equal to one, so that only pure CO₂ phase would enter the brine-saturated column. We augmented this

Table 1. Properties of the of the LUCI system.

Property	Value
Porosity (ϕ)	0.40
Permeability (k)	$1.7 \times 10^{-11} \text{ m}^2$
Capillary Pressure (P_{cap}) and Relative Permeability (k_r)	van Genuchten ¹ two-phase and Parker ² three-phase
<i>Terminology:</i>	$\lambda = 0.774$
$\lambda = m = 1 - 1/n =$ power in expressions for P_{cap} and k_r	$S_{ar} = 0.127$ for P_{cap} , 0.130 for k_r
$S_{ar} = S_m =$ aqueous-phase residual saturation	$S_{lr} = 0$
$S_{lr} =$ CO ₂ liquid-phase residual saturation	$S_{gr} = 0.01$
$S_{gr} =$ CO ₂ gas-phase residual saturation	$P_{c0} = 2875 \text{ Pa}$
$P_{c0} = \alpha' =$ capillary pressure between aqueous and non-aqueous phases	$P_{cmax} = 1 \times 10^6 \text{ Pa}$
$P_{cmax} =$ maximum possible value of P_{cap}	P_{cap} between CO ₂ gas, liquid, and supercritical phases is assumed to be zero.
Thermal conductivity of sand and brine mixture ⁴	2.5 W/(m K)
Thermal conductivity of 5 cm-thick stainless steel (304) on RHS boundary	14.6 W/(m K)
Density of stainless steel	7920 kg/m ³
Heat capacity (C_p) of stainless steel	502.1 J/(kg K)

¹van Genuchten (1980), as in Doughty (2007)

²Parker et al. (1987) as in Pruess (2011), simplifies to van Genuchten when only two phases present

injection rate by a factor of two above the pure buoyant rate to make a flow system that would evolve on a relatively short time scale convenient for the experimentalists who would be operating LUCI. The CO₂ injected at the bottom is into a row of gridblocks with infinite heat capacity, which implements a constant-temperature injection.

RESULTS

Fixed geothermal gradient boundary

In this scenario, CO₂ is injected at a constant rate and temperature into the bottom of the LCPV, which is initially filled with a brine with 100,000 ppm NaCl at hydrostatic pressure and temperature equal to the selected geothermal gradient. Temperature at the outer wall or RHS boundary is held fixed at this geothermal gradient profile. Figure 3 shows results at $t = 5$ d following the start of injection. As shown, the CO₂ front has moved upwards approximately 260 m, creating a region of two-phase gaseous and super-critical CO₂ (scCO₂)-brine mixture. The pressure in the system increases due to this injection process. Isotherms are generally lifted upwards as the brine is displaced upwards and the injected CO₂ is at the relatively warmer temperature of the bottom boundary. The injected CO₂ decompresses as it rises upward through the hydrostatic pressure of the brine column and may exchange heat with the outer wall of the column. Overall, the simulation shows some minor two-dimensional effects arising from the fixed geothermal gradient boundary condition.

The nearly one-dimensional nature of the flow problem allows us to plot results as vertical profiles through the system. Figure 4 shows values of P , T , S_{CO_2} , and ρ_{CO_2} for vertical profiles along the LHS of the LCPV at four times to explicitly show the vertical variations in temperature and phase conditions in the system—for example, the clear indication of the phase front. Note also that we include the liquid-gas phase boundary in the temperature plot. This curve represents the locus of points along which gas and liquid CO₂ are in equilibrium at the given pressure of the system. At $t = 5$ d, the CO₂ is supercritical below approximately -320 m and gaseous above. The effects of expansion cooling at $t = 5$ d can be seen clearly on the vertical profile plots of Figure 4 by the deflection toward lower temperatures at around $z = -350$ m and near-intersection with the liquid-gas phase boundary. The increased T relative to initial condition between $z = -250$ m and -350 m is likely due to advection of warmer fluid upward.

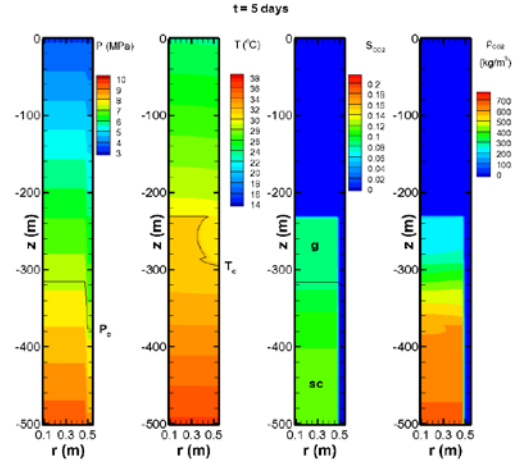


Figure 3. Results at $t = 5$ d showing P , T , S_{CO_2} , and ρ_{CO_2} for the case of the fixed geothermal gradient boundary condition on the RHS. The critical pressure (P_c) and temperature (T_c) are indicated by the light solid curves on the P and T plots.

Insulated boundary

To understand the effect of the outer wall (RHS) thermal boundary condition, we consider next a case identical to the above except the RHS (outer wall) is perfectly insulated. Results at $t = 5$ d are shown in Figure 5 for comparison to Figure 3. The first observation is that the system behaves essentially like a one-dimensional system in terms of fluid (P) and heat (T) flow with no lateral variation whatsoever. Second, with no heat entering or leaving through the RHS boundary, the intrinsic thermal effects are more obvious, because they are controlled solely by advection, conduction, expansion, and phase change effects.

Vertical profiles of results for $t = 5$ d, 10 d, 20 d, and 30 d are shown in Figure 6. As shown, interesting oscillations in temperature occur at various times, resulting in liquid CO₂ conditions alternating with scCO₂ and gaseous CO₂. The occurrence of liquid CO₂ causes phase interference that impedes upward flow and introduces a negative feedback to the expected expansion cooling, resulting in oscillations in density and temperature.

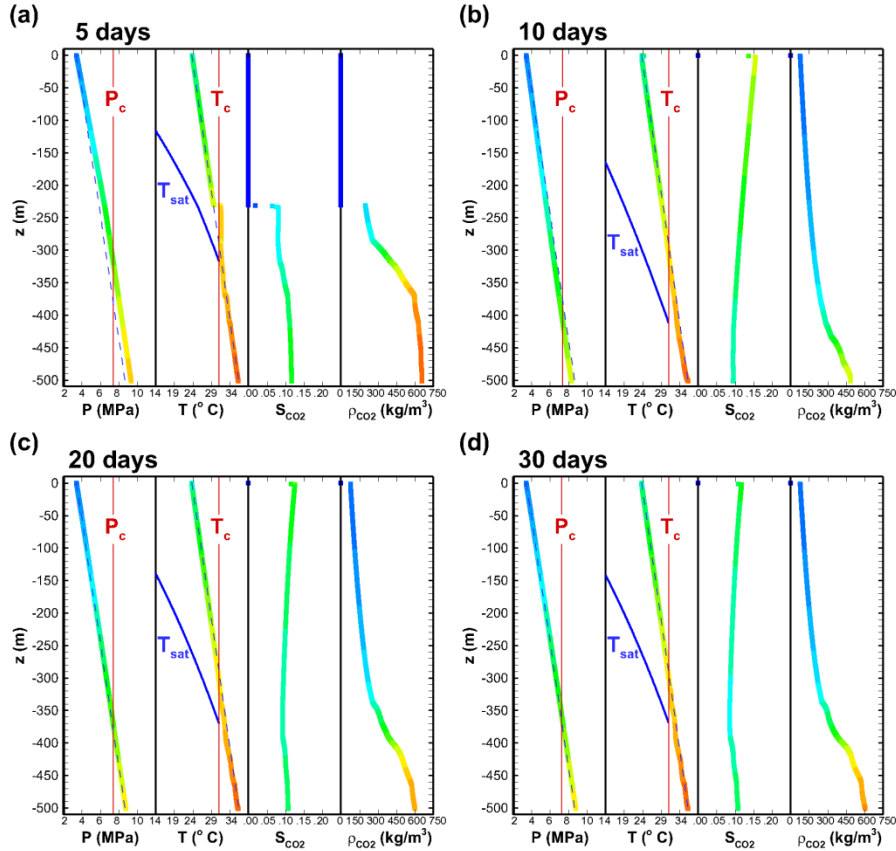


Figure 4. Vertical profiles along the inner radius of the domain at (a) $t = 5$ d, (b) $t = 10$ d, (c) $t = 20$ d, and (d) $t = 30$ d for the fixed geothermal gradient boundary condition on the RHS. The color of the lines represents the value of the variable being plotted against depth, for visual emphasis. Initial conditions for P and T are shown by the dashed lines. The liquid-gas phase boundary is shown in the temperature frame by the line labeled T_{sat} .

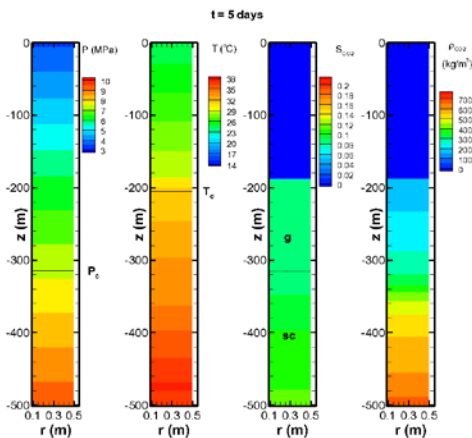


Figure 5. Results for the case with an insulated boundary condition on the RHS. Note that there is no variation in the lateral (r) direction (i.e., the fields are one-dimensional)

At $t = 30$ d, liquid CO_2 is present from $z = -200$ m to -370 m. The large region of liquid CO_2 points to the importance of expansion cooling in large-scale buoyant CO_2 rise, at least for systems with high porosity and permeability. At the liquid-gas phase boundary, there are two CO_2 phases (liquid and gas) in equilibrium with an aqueous phase. In this situation, three-phase relative permeability and capillary pressure functions are needed. The migration of the system to the liquid-gas phase boundary seems to be a fundamental behavior of the system observed for all reasonable combinations of relative permeability tested so far. To see alternative graphical and animated representations of these simulation results, please see animated time plots in the Supplementary Material of our *Greenhouse Gases: Science and Technology* paper (Oldenburg et al., 2011).

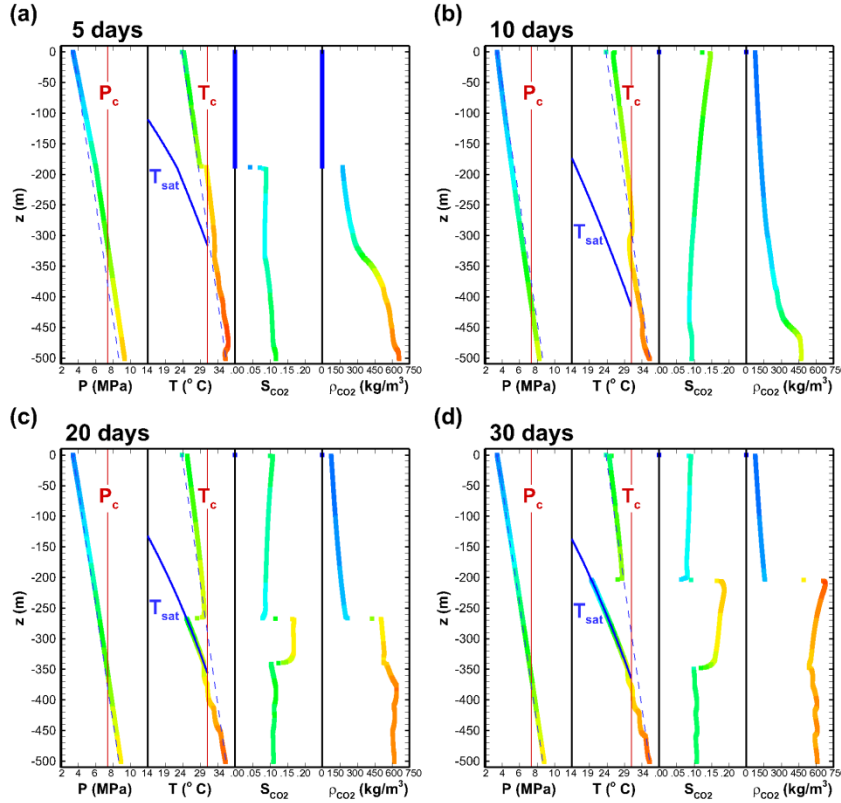


Figure 6. Vertical profiles along the inner radius of the domain at (a) $t = 5$ d, (b) $t = 10$ d, (c) $t = 20$ d, and (d) $t = 30$ d for the case with insulated boundary condition on the RHS.

CONCLUSIONS

Numerical simulations using TOUGH2/ECO2M for the preliminary design of long-column flow experiments such as those proposed for LUCI have been carried out. The fixed geothermal gradient boundary condition is representative of the case of CO_2 flow up a narrow conduit such as the annulus of an abandoned well or a fault zone. The insulated boundary condition is representative of the upward flow of CO_2 in the middle of a much larger CO_2 plume. Simulation results for scenarios involving constant injection of CO_2 in an initially brine-filled sand column are sensitive to the outer wall thermal boundary condition. Radial gradients in temperature occur for the fixed geothermal gradient case, showing that the outer wall temperature controls the temperature in the system, whereas in the insulated case, heat transfer and temperature are controlled by vertical advection and conduction, expansion, and phase-change processes.

Liquid CO_2 forms in flow simulations using either boundary condition, but much more liquid forms in the insulated outer wall case, because

expansion cooling is stronger when the outer wall boundary does not supply heat to the system. When two-phase liquid-gas conditions occur, the system becomes locked onto the liquid-gas phase boundary. The prevalence of liquid CO_2 in these upward-leakage simulations and the lack of knowledge about modeling three-phase relative permeability motivate the development of a large-scale experimental facility with LCPVs, in which controlled flow experiments can be carried out. An experimental facility would provide the opportunity for researchers to investigate outstanding research questions, such as the role of phase interference in multiphase CO_2 systems along with much more realistic and complex systems—for example, by layering different materials into the column, and including reactive transport and other physical and chemical processes. In all likelihood, a large-scale experiment would reveal additional unpredicted behaviors, the study of which could allow increased understanding of large-scale flow and phase change phenomena in CO_2 systems.

ACKNOWLEDGMENT

This work was supported by the National Science Foundation under Grant Numbers CMMI-0965552 (to LBNL) & CMMI-0919140 (to Princeton University), and by Lawrence Berkeley National Laboratory under Department of Energy Contract No. DE-AC02-05CH11231.

REFERENCES

- De la Reguera D, Stute M, Matter JM. Laboratory experiments on CO₂ dissolution in water for carbon sequestration. Proceedings of the American Geophysical Union EOS, 2010 Dec 13-17, San Francisco, CA (2010).
- Doughty C. Modeling geologic storage of carbon dioxide: Comparison of non-hysteretic and hysteretic characteristic curves. *Energy Conversion and Management* 48(6): 1768–1781 (2007).
- Gasda SE, Bachu S, Celia MA. Spatial characterization of the location of potentially leaky wells penetrating a deep saline aquifer in a mature sedimentary basin. *J Environ Geol* 46(6-7): 707-720 (2004).
- Maloney DR, Briceno M. Experimental investigation of cooling effects resulting from injecting high pressure liquid or supercritical CO₂ into a low pressure gas reservoir. Proceedings of the International Symposium of the Society of Core Analysts held in Abu Dhabi, UAE, 29 October-2 November 2008.
- Oldenburg, C.M., C. Doughty, C.A. Peters, and P.F. Dobson, Simulations of long-column flow experiments related to geologic carbon sequestration: effects of outer wall boundary condition on upward flow and formation of liquid CO₂, *Greenhouse Gases: Science and Technology*, in press.
- Parker JC, Lenhard RJ, Koppusamy T. A parametric model for constitutive properties governing multiphase flow in porous media. *Water Resources Research* 23(4): 618- 624 (1987).
- Peters CA, Dobson PF, Oldenburg CM, Wang JSY, Onstott TC, Scherer GW, et al. LUCI: A facility at DUSEL for large-scale experimental study of geologic carbon sequestration. *Energy Procedia*, 2, Elsevier, GHGT-10, Sept. 19–23, 2010, Amsterdam, The Netherlands (2010).
- Pruess K. On CO₂ fluid flow and heat transfer behavior in the subsurface, following leakage from a geologic storage reservoir. *J Environ Geol* 54: 1677-1686 (2007).
- Pruess K. Integrated modeling of CO₂ storage and leakage scenarios including transitions between super- and subcritical conditions, and phase change between liquid and gaseous CO₂. *Greenhouse Gases: Science and Technology* 1(3): 237–247 (2011).
- Pruess K. ECO₂M: A TOUGH2 fluid property module for mixtures of water, NaCl, and CO₂, including super- and sub-critical conditions, and phase change between liquid and gaseous CO₂. May 2011, Lawrence Berkeley National Laboratory Report LBNL-4590E (2011).
- Pruess K, Oldenburg CM, Moridis GJ. TOUGH2 User's Guide Version 2. November 1999, Lawrence Berkeley National Laboratory Report LBNL-43134 (1999).
- Schaap MG. Rosetta Version 1.2. U.S Salinity Laboratory ARS-USDA (2000).
- Stauffer P, Stein J, Travis B. The correct form of the energy balance for fully coupled thermodynamics in water. Los Alamos National Laboratory Report LA-UR-03-1555, 9 pp (2003).
- van Genuchten M Th. A closed-form equation for predicting the hydraulic conductivity of unsaturated soils. *Soil Science Society of America J* 44(5): 892–898 (1980).